materials proceedings

MDPI

Proceeding Paper

Synthesis and Characterization of Nanocomposites Based on Carbon Materials and Transitional Oxides †

Vasilica Țucureanu *, Cosmin Alexandru Obreja, Cristina Pachiu, Oana Brîncoveanu and Alina Matei *

National Institute for Research and Development in Microtechnologies, IMT-Bucharest, 126A Erou Iancu Nicolae Street, 077190 Bucharest, Romania; email1@email.com (C.A.O.); email2@email.com (C.P.); email3@email.com (O.B.)

* Correspondence: vasilica.tucureanu@imt.ro (V.Ț.); alina.matei@imt.ro (A.M.)

† Presented at the 4th International Online Conference on Nanomaterials, 5–19 May 2023; Available online: https://iocn2023.sciforum.net.

Abstract: The use of nanostructured materials in the biomedical field aims for diagnostics, drug delivery, therapy activation and monitoring therapeutic responses in real-time, thus maximizing the therapeutic benefits, simultaneously with a minimally invasive effect and low toxicity. Electrochemical analysis and implicitly the development of materials for biosensors have become of vital importance for the monitoring of biomolecules. The conductivity of nanocomposites is usually determined by characteristics related to the concentration, size, and dispersion of the nanoparticles. Generally, graphene's high surface energy and strong interactions moderate its uniform compatibility with different media. In the present paper, we propose the synthesis of yttrium oxide nanoparticles for developing nanocomposites based on transition oxides and carbon materials for electrochemical applications. The precipitation method was used to obtain nanostructured Y_2O_3. The Hummer method was used for the synthesis of graphene material. After the activation step of the Y_2O_3 surface, the ex-situ method was chosen to obtain the nanocomposites, allowing the insertion of oxide nanoparticles into the sheets of carbon materials. The developed materials were studied from a structural point of view using Raman and FTIR spectroscopy. The surface morphology, particle size and distribution of nanoparticles in the carbon material were studied using a field emission scanning electron microscope. The goniometric studies followed the wetting and percolation capacity of the nanocomposite.

Keywords: carbon materials; transitional oxides; Y_2O_3; graphene; nanocomposites; RGO-Y_2O_3

Citation: Țucureanu, V.; Obreja, C.A.; Pachiu, C.; Brîncoveanu, O.; Matei, A. Synthesis and Characterization of Nanocomposites Based on Carbon Materials and Transitional Oxides. *Mater. Proc.* **2023**, *14*, x. https://doi.org/10.3390/xxxxx

Published: 5 May 2023

1. Introduction

Nanotechnology has gained fundamental importance in the development of biomedical systems, due to the fact that nanostructured materials present unique properties and dimensions appropriate to many biological systems, their use is expected to bring revolutionary changes in medical diagnosis and therapy with minimal damage. For the detection of biomolecules, although there are many analysis techniques, the development of fast, cheap, and accessible detection methods is desired. In this regard, electrochemistry has registered many advances as a result of the development of materials that have allowed the improvement of reproducibility, the reduction of detection limits and the ease in the detection of the analyte of interest. In recent decades, nanomaterial composite systems have attracted significant interest, as they combine different types of materials into a single multifunctional nanostructure, which exhibits the properties of its component modules. Nanostructured composites based on carbon materials and transitional metals have become a topical area with multiple applications. Nanomaterial-based sensors offer a new class of fast, reliable, selective etc. detectors at a low cost. Additionally, carbon materials have begun to be used more and more in the development of

electrodes for various applications due to their unique structure and extraordinary electronic properties. Carbon materials (CNT, RGO, etc.) have a large surface area, significant mechanical strength, high electrical conductivity and efficient electrocatalytic activity. It is known that the attachment of inorganic nanoparticles on graphene can inhibit aggregation and significantly improve the persuasive effect on the electrochemical properties by attaching them to the surface of the carbon material [1,2]. Yttrium oxide nanoparticles (Y_2O_3) are mechanically, chemically and thermally stable, have a narrow bandgap that allows electron transfer and provide excellent electrochemical sensitivity [3,4]. However, the literature presents few data regarding the realization of microsensors based on Y_2O_3. Studies have been found regarding the realization of sensors based on PVA-Y_2O_3:Eu composite designed for the non-enzymatic detection of H_2O_2 in biological environments. By using the GO-Y_2O_3 or CNT-Y_2O_3 type composites, studies were conducted for detecting acetaminophen, and with the RGO-Y_2O_3:Cr^{3+} nanocomposite for detecting dopamine [1,4,5].

In the present paper, we propose the synthesis of Y_2O_3 and RGO nanoparticles for the development of nanocomposites based on transition oxides and carbon materials for integration in electrochemical applications. The materials are characterized from structural and morphological point of view using FTIR spectrometry, Raman spectrometry, and SEM. The goniometric studies followed the wetting and percolation capacity of the nanocomposite. The knowledge obtained from the study provides a better understanding of the synthesis steps of high-purity nanomaterials to develop electrochemical sensors for detection in biomedical applications.

2. Experimental

2.1. Synthesis of Carbon Material

Reduced graphene oxide (RGO) was prepared using Hummer's method by oxidizing graphite with sulfuric acid (H_2SO_4), sodium nitrate ($NaNO_3$) and potassium permanganate ($KMnO_4$) [6,7]. Followed by neutralization with hydrogen peroxide (H_2O_2) and purification in the presence of hydrochloric acid (HCl). The reduction of graphene oxide is carried out with hydrazine in the presence of N-methyl-2-pyrrolidone (C_5H_9NO). At the end, steps of decanting, washing with ethanol, redispersion were repeated, for the purification of RGO.

2.2. Synthesis of Oxide Nanoparticles

To obtain the oxide precursor, a mixture of acetyl acetone ($C_5H_8O_2$) and dimethyl sulfoxide (C_2H_6OS) was added over the yttrium nitrate solution ($Y(NO_3)_3 \cdot 6H_2O$). Acetyl acetone acts as a chelating agent. Stirring and heating are started, under reflux conditions, and ethylene glycol ($C_2H_6O_2$) and CTAB ($C_{19}H_{42}BrN$) surfactant are added. Ethylene glycol ($C_2H_6O_2$) acts as a stabilizing agent, allowing the binding of the chelating agent through polyesterification reactions, and favors the formation of the gel. During the process it was found that the hydrolysis and condensation steps are favored by keeping the pH constant at the value of 4–5, it is undesirable to increase the pH, in this case flocculation and the formation of an unwanted precipitate may occur. Nitric acid (HNO_3) was used to adjust the pH. After 3 h, reflux conditions were removed, stirring and heating were stopped, it is left to mature for polymerization and gel formation. The final thermal treatment occurs at 900 °C for 6 h.

2.3. Synthesis of Nanocomposite

In the first part of the synthesis process of the Y_2O_3-RGO composite, the oxide is dispersed in hydrogen peroxide to form OH groups on the surface, then it is subjected to repeated steps of centrifugation-decantation-washing-redispersion in ethanol. RGO is added to the previous solution. To favor a good insertion of the oxide nanoparticles between the RGO sheets, ultrasonication is used for 4 h, at 45 kHz.

3. Results and Discussion

The physico-chemical properties and applicable capacity of Y_2O_3 nanoparticles in the biomedical field are strongly influenced by the morphology and structure of the particles. Figure 1 shows the comparative ATR-FTIR spectra taken for oxid precursor, Y_2O_3 nanoparticles after the surface activation stage, RGO and the Y_2O_3-RGO composite. The spectrum of the oxide is characterized by absorption bands that can be associated with Y-O bonds from Y_2O_3 (564 cm^{-1}), and OH bonds anchored to the oxide surface (3432 cm^{-1}). In the spectra of the composites, the existence of the characteristic peak of Y-O bonds can be observed, but with a very slight shift of it towards lower wavenumbers (560 cm^{-1}) compared to the oxide nanoparticles and the disappearance of the OH band, as a result of the interference with the carbon material. In IR spectroscopy, the RGO does not show any specific absorption band, is the reason why the presence of RGO in composites was studied using Raman spectroscopy [5,8–11].

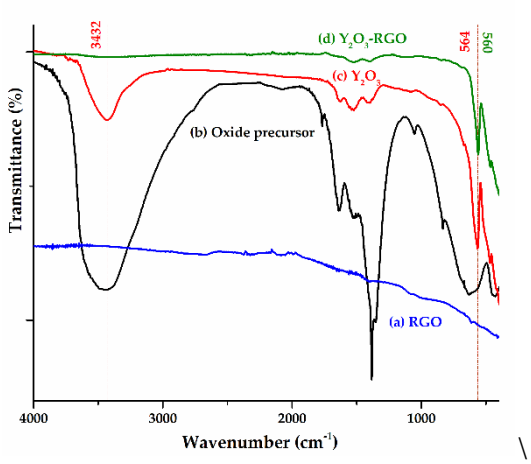

Figure 1. ATR-FTIR spectra for samples of (a) RGO, (b) oxide precursor, (c) Y_2O_3 after surface activation and (d) Y_2O_3-RGO composite**.**

Figure 2 shows the Raman spectra for the RGO and the Y_2O_3-RGO nanocomposite. The Raman spectrum plotted for RGO is characterized by two bands centered at 1581 cm^{-1}, the maximum assigned to a G band that confirms the graphitic nature of the filler, and respectively 1345 cm^{-1}, the D band that can be associated to the sp^2 carbon out-of-plane vibration from graphene. In the spectra of the Y_2O_3-RGO composite, the existence of similar peaks can be observed, but with a slight shift, broadening of the bands and an increase in the intensity of the peaks as a result of the insertion of the oxide between the graphene sheets [5,8,10].

The SEM image in Figure 3a for the Y_2O_3 sample highlights the formation of agglomerated particles, without defects on the surface, for which an average particle size of 30–40 nm was found. In Figure 3b, the SEM image for the Y_2O_3-RGO composite can be seen, confirming the formation of the nanocomposite, a close interaction between the main components of the composite where the RGO nanosheets are well interposed with oxide nanoparticles.

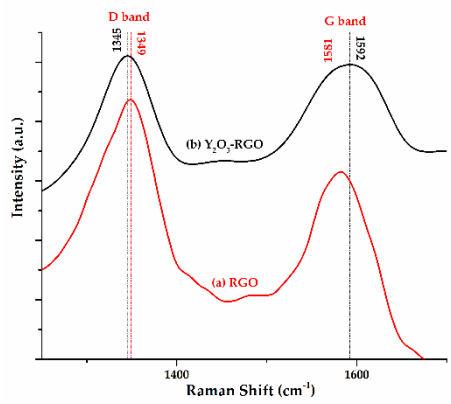

Figure 2. Raman spectra for the sample of (a) RGO and (b) Y_2O_3-RGO nanocomposite.

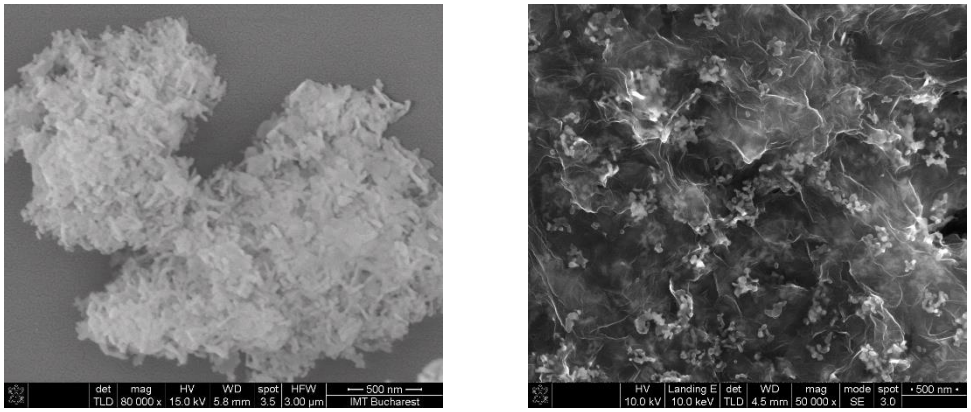

(**a**) (**b**)

Figure 3. SEM images for (**a**) Y_2O_3 nanoparticles and (**b**) Y_2O_3–RGO composite.

The wetting capacity of a film is determined by the chemical composition and morphology of the surface, and is reflected in the value of the contact angle when the water interacts with the surface of the composite film. Figure 5 shows the values of water contact angles obtained for a Y_2O_3-RGO composite film, measured in the interval 0–30 sec after the drop water comes into contact with the composite film. A hydrophilic character was found for the composite, which can be attributed to the insertion of Y_2O_3 particles between the RGO sheets and the interaction with them. The percolation capacity of the composites is supported by the decrease of the contact angle with increasing time [6].

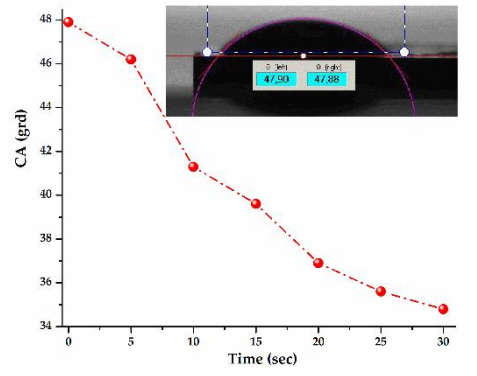

Figure 4. The variation of the contact angle depending on the time elapsed since the contact of the water droplet with the Y_2O_3-RGO nanocomposite.

4. Conclusions

Y_2O_3 nanoparticles were obtained by the sol-gel method, RGO using the Hummer method, and the Y_2O_3-RGO nanocomposite by ex-situ process was obtained. The FTIR spectrum confirms the formation of Y_2O_3, and in the case of the composite, the existence of the characteristic Y-O peak is observed, but with a slight shift of it toward lower wave numbers compared to the raw material, as a result of the interference with the carbon material. The Raman spectrum plotted for RGO is characterized by two peaks that show the graphitic nature of the carbon material (band G), and respectively the sp^2 carbon from graphene (band D). In the spectra of the Y_2O_3-RGO composite, the existence of these peaks is confirmed, with a slight shift due to the insertion of the oxide between the RGO sheets. The SEM images confirm the nanostructuring of Y_2O_3 particles, and for the Y_2O_3-RGO composite it shows the uniform dispersion of the fillers, the insertion of the Y_2O_3 nanoparticles into the RGO sheets and the close interaction between the components of the composite. The contact angle is lower than 90°, confirming the obtaining of a hydrophilic composite with good percolation capacity.

Author Contributions: V.Ț. conceived, planned, carried out the experiments for Y_2O_3 and composite synthesis and FTIR characterization. C.A.O. carried out the experiments for RGO synthesis. O.B. performed SEM characterization, C.P. did Raman characterization, and A.M. the wettability studies. V.Ț. wrote the manuscript with support from A.M. All authors have read and agreed to the published version of the manuscript.

Acknowledgments: This work was supported by Core Program within the National Research Development and Innovation Plan 2022–2027, carried out with the support of MCID, project no. 2307 (μNanoEl).

Conflicts of Interest: The authors declare no conflict of interest.

References

1. Shashikumara, J.K.; Kalaburgi, B.; Kumara Swamy, B.E.; Nagabhushana, H.; Sharma, S.C.; Lalitha, P. Effect of RGO-Y_2O_3 and RGO-Y_2O_3:Cr^{3+} nanocomposite sensor for dopamine. *Sci. Rep*. **2021**, *11*, 9372. https://doi.org/10.1038/s41598-021-87749-z.
2. Loh, K.P.; Bao, Q.; Ang, P.K.; Yang, J. The chemistry of graphene. *J. Mater. Chem*. **2010**, *20*, 2277. https://doi.org/10.1039/B920539J.
3. Kumar, S.; Panwar, S.; Kumar, S.; Augustine, S.; Malhotra, B.D.; Biofunctionalized Nanostructured Yttria Modified Non-Invasive Impedometric Biosensor for Ecient Detection of Oral Cancer. *Nanomaterials* **2019**, *9*, 1190. https://doi.org/10.3390/nano9091190.
4. Rajakumar, G.; Mao, L.; Bao, T.; Wen, W.; Wang, S.; Gomathi, T.; Gnanasundaram, N.; Rebezov, M.; Shariati, M.A.; Chung, I.M.; et al. Yttrium Oxide Nanoparticle Synthesis: An Overview of Methods of Preparation and Biomedical Applications. *Appl. Sci*. **2021**, *11*, 2172. https://doi.org/10.3390/app11052172.
5. Sánchez, C.M.; Montiel-González, F.; Rodríguez-González, V.; Electrochemical sensing of acetaminophen using a practical carbon paste electrode modified with a graphene oxide-Y_2O_3 nanocomposite. *J. Taiwan Inst. Chem. Eng.* **2019**, *96*, 382–389. https://doi.org/10.1016/j.jtice.2018.12.004.
6. Tucureanu, V.; Obreja, C.A.; Craciun, G.; Romanițan, C.; Mihailescu, C.M.; Stan, D.; Matei, A.; Preparation and evaluation of nanocomposites based on transitional oxides and carbon materials for electrochemical applications. *Ceram. Int.* **2022**, *48*, 27201–27212. https://doi.org/10.1016/j.ceramint.2022.06.032.
7. Obreja, A.C.; Cristea, D.; Gavrila, R.; Schiopu, V.; Dinescu, A.; Danila, M.; Comanescu, F. Functionalized graphene/poly 3-hexyl thiophene based nanocomposites. In Proceedings of the CAS 2011 Proceedings, Sinaia, Romania, 17–19 October 2011; pp. 27–30. https://doi.org/10.1109/SMICND.2011.6095703.
8. Saravanan, T.; Anandan, P.; Azhagurajan, M.; Arivanandhan, M.; Pazhanivel, K.; Hayakawa, Y.; Jayavel, R.; Synthesis and characterization of Y_2O_3-reduced graphene oxide nanocomposites for photocatalytic applications. *Mater. Res. Express* **2016**, *3*, 075502. https://doi.org/10.1088/2053-1591/3/7/075502.
9. Munawar, T.; Mukhtar, F.; Nadeem, M.S.; Mahmood, K.; Hussain, A.; Ali, A.; Arshad, M.I.; Ajaz un-Nabi, M.; Iqbal, F.; Structural, optical, electrical, and morphological studies of rGO anchored direct dual-Z-scheme ZnO-Sm_2O_3–Y_2O_3 heterostructured nanocomposite: An efficient photocatalyst under sunlight. *Solid State Sci.* **2020**, *106*, 106307. https://doi.org/10.1016/j.solidstatesciences.2020.106307.
10. Mandal, G.; Choudhary, R.B. rGO–Y_2O_3 intercalated PANI matrix (PANI–rGO–Y_2O_3) based polymeric nanohybrid material as electron transport layer for OLED application, *Res. Chem. Intermed*. **2019**, *45*, 3755. https://doi.org/10.1007/s11164-019-03819-y.

11. Tucureanu, V.; Matei, A.; Avram, A.M. FTIR Spectroscopy for Carbon Family Study, *Crit. Rev. Anal. Chem*. **2016**, *46*, 502–520. https://doi.org/10.1080/10408347.2016.1157013.